Egypt. J. Chem. **Vol. 66,** No. **SI 13, 1069-1079** (2023)

Egyptian Journal of Chemistry

http://ejchem.journals.ekb.eg/

Corrosion Inhibition of Hybrid Ti/Ce Salt for Zinc in HCl Solution

Aliaa Abdelfatah, [a] Lamiaa Z. Mohamed, [a,*] Ghalia A. Gaber, [b]

[a]*Mining, Petroleum, and Metallurgical Engineering Department, Faculty of Engineering, Cairo University, 12613, Giza, Egypt*

[b]*Department of Chemistry, Faculty of Science (Girls), Al-Azhar University, P.O. Box: 11754, Yousef Abbas Str., Nasr City, Cairo, Egypt*

Abstract

The inhibition of zinc of hybrid Ti/Ce salt with 0, 100, 300, 600, 900, 1200, and 1600 ppm concentrations was investigated by weight-loss (WL) estimation and potentiodynamic polarization (PDP) in 1M HCl solution. The inhibition efficiency of hybrid Ti/Ce salt was evaluated as a corrosion inhibitor by immersing the Zn in it over a period extending up to 120 h and the temperature effect (25-55 ºC) on inhibition of Zn. WL and the corrosion rate (C_R) were recorded after a short immersing time and 120 h of immersion. A passive layer was formed after 24 h at a high concentration of 1600 ppm hybrid Ti/Ce salt and was stable till 120 h. The surface morphology and composition of the different investigated conditions were studied by SEM and EDX analysis, respectively.

Keywords: Zinc; inhibition; Corrosion behavior; HCl; Microstructure.

1. Introduction

Corrosion damage is a severe problem in the industry due to its cost and environmental issues that decrease the efficiency of the metal [1, 2]. Zinc is a commonly employed essential non-ferrous metal that is widely used in coating metals especially steel [3, 4]. Rapid corrosion for Zn and Zn-coated products are formed a white corrosion product in most corrosive environments thus it must also be protected from corrosion by inhibitors [5, 6]. A high corrosion rate (C_R) of Zn in the corrosive solution that has a pH lower than 6.0 or higher than 12.5 [7] could be protected in acidic media by using inhibitors [8, 9]. Several researchers were researching the effect of organic additives on the C_R of Zn in acid solutions [10]. It has been known that these compounds on the metallic surface form a protective film that isolates the corroded metal from the media of corrosion. Schiff bases are also employed in different media as effective corrosion inhibitors [11]. Most compounds regulate corrosion by the metal ion complex formation by adding to them solutions of complexing agents. Several studies are related to the alteration of the metal surface by complicating it with organic compounds [12]. The key criterion for choosing them as surface modifiers was the complex forming potential of organic compounds with Zn by immersion for a definite duration in this modification process [13]. A few microns of metal surface thickness can be shielded into metal chelates or metal complexes during the contract which serves as a buffer between the metal surface and media of corrosion [14, 15]. Highly corrosive media such as HCl solutions are employed for several such as pickling, and cleaning zinc surfaces [16, 17, 18]. The Ce^{3+} ions react easily to form a protective film on the Al surface of complex hydrated Ce-oxides [19]. This oxide film decreases the oxygen reduction rate on the metal surface at cathodic locations, thus reducing the C_R [20, 21]. There are many parallels between Al and Zn from a corrosion perspective such as covered by an oxide film that is soluble in high and low pH solutions. As corrosion inhibitors, rare earth salts are especially desirable because they are inexpensive and non-toxic. It investigated the TiC and TiO_2 doping in coating to improve the corrosion resistance of the substrate [22]. Also, the TiN/TiO_2 nanoparticles have a high corrosion resistance on Mg alloy [23]. Thus, doping of TiO_2 and CeO_2 has excellent corrosion behavior as corrosion inhibitors.

The target of this research is to study the effectiveness of hybrid Ti/Ce salt as an inhibition efficiency for Zn in 1M HCl acidic media using the WL method and

*Corresponding author e-mail: lamiaa.zaky@cu.edu.eg ; (Lamiaa Z. Mohamed).

Receive Date: 27 March 2023, Revise Date: 02 May 2023, Accept Date: 07 May 2023

DOI: 10.21608/EJCHEM.2023.202393.7785

potentiodynamic polarization (PDP). The inhibitor was added to Zn from 0 to 1600 ppm concentrations of hybrid Ti/Ce salt and tested at various time intervals and temperatures (25-55 ºC) in 1M HCl solution and evaluate its efficiency against corrosion. The surface morphology and composition by scanning electron microscopy (SEM) and energy dispersive x-ray analysis (EDX) were investigated in the Zn surface protective film produced after immersion in 1M HCl with different concentrations of hybrid Ti/Ce salt.

2. Experimental work

The Zn samples with 2 cm x 2 cm plates were explored as a sample to investigate the inhibition behavior in different Ti/Ce salt concentrations. The Zn samples were ground with SiC emery papers up to 1000 grids and then polished by alumina paste 0.3 µm. The plates were cleaned with double distilled water, degreased with acetone, dried, and weighed [24].

The hybrid composition includes cerium sulphate of 33.2 g/L (source of Ce), and 4.8 g/L of pure Ti powder (99.9%) with a particle size of about 2 µm as shown in Fig. 1. The figure gives the Ti morphology and elemental composition (100%Ti). These additives were chemically pure grades and obtained from Aldrich.

The weight loss (WL) technique was adopted to examine the inhibition behavior of the Zn surface with a 4 cm^2 surface area. The previously weighed plates were immersed in 50 ml of different concentrations of Ti/Ce salt (0, 100, 300, 600, 900, 1200, and 1600 ppm). The immersion was continued for up to 120 h at room temperature. Throughout the WL tests, Zn plates were weighted (W_1) and suspended completely in 1M HCl solution in different concentrations of the investigated inhibitor. After 0.5, 1, 2, 3, 4, 24, 48, 72, 96, and 120 h, plates were gotten out of the solution, washed, dried with acetone, and reweighed (W_2). The weight difference of the specimens before and after exposure is demonstrated in Eq. 1, and the $\boldsymbol{C_R}$ is calculated from Eq. 2 [25, 26].

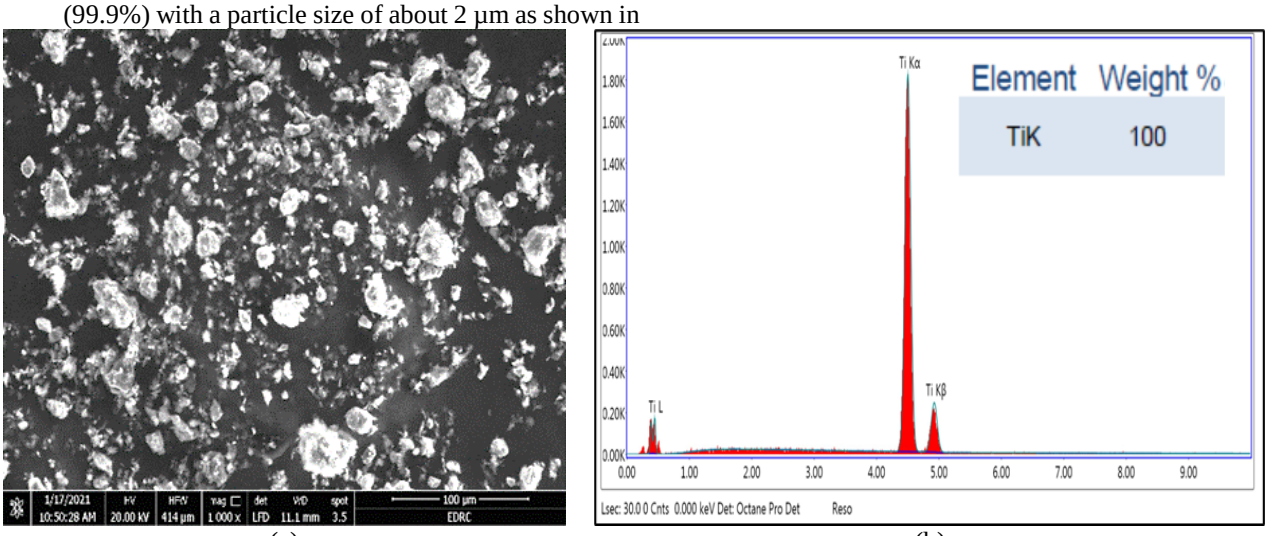

(a) (b)

Fig. 1 The Ti powder (a) SEM and (b) EDX

$$\Delta W = W_1 - W_2 \quad (1)$$

$$C_R\ (mm/y) = \frac{\Delta W * K}{A * T * D} \quad (2)$$

where K denotes a constant ($8.76x10^4$), T denotes the time of exposure in h, A denotes area in cm^2 (2cm x 2cm), ΔW denotes weight-loss in grams, and D denotes density in g/cm^3 (7.140 for Zn). The inhibition efficiency (IE) and surface coverage (θ) are given by Eqs. 3 and 4:

$$IE\ (\%) = \left(\frac{C_{R_0} - C_{R_{inh}}}{C_{R_0}}\right) * 100 \quad (3)$$

Where C_{R_0} and $C_{R_{inh}}$ are the C_R of Zn in the existence and without of inhibitor, separately [27].

$$Surface\ coverage\ (\theta) = IE/100 \quad (4)$$

The PDP curves of zinc were swept potential between -1500 mV/REF to + 600 mV/REF at the scan rate of 0.5 mV/s. Before the measurements were occupied, the working electrode was immersed in the test solution for 30 min to achieve a quasi-stationary value of the open circuit potential. Values of I_{corr} and corrosion potential (E_{corr}) were assessed from the intersection of the linear anodic and cathodic branches of Tafel plots and were designed with and without different concentrations of hybrid Ti/Ce salt. The polarization resistance (R_p) values are demonstrated using Stern–Geary Eq. 5 [28]:

$$R_P = \frac{\beta_a * \beta_c}{2.303\, I_{corr}\,(\beta_a + \beta_c)} \quad (5)$$

Degrees of surface coverage (θ) in PDP measurements are calculated using Eq. 6.

$$\theta = 1 - I_{corr}/I^{\circ}_{corr} \quad (6)$$

where I°_{corr} and I_{corr} are the corrosion current densities in the absence and presence of hybrid Ti/Ce salt, respectively. The inhibitive efficiency (IE %) is calculated employing Eq. 7:

$$IE\,\% = \theta * 100 \quad (7)$$

The surface morphology of the corroded Zn surfaces and elemental analyses were characterized by SEM and EDX.

3. Results and Discussion

3.1. Effect of Inhibitor Concentration

The efficiency of inhibitor attributed to its structure, electrolyte composition, and the charge on the metal surface [29]. The inhibition efficiency rate percentage (IE %) and $\boldsymbol{C_R}$ were calculated from the WL at various concentrations of hybrid Ti/Ce salt at 25 °Cas shown in Table 1 and Fig.2. At 1600 ppm, it has the lowest $\boldsymbol{C_R}$ because of the protective film formation and lowering of the effective electron transfer rate at the interface. The Zn corrosion in 1 M HCl is inhibited by the addition of hybrid Ti/Ce salt at different concentrations used in this study 0 to 1600 ppm.

Table 1. The WL values of Zn in 1M HCl without and presence of different hybrid Ti/Ce salt concentrations at 25 °C after 4 h and 120 h.

Conc. of inhibitor (ppm)	After 4 h				After 120 h			
	WL, (g)	$\boldsymbol{C_R}$, (mm/Y)	Coverage surface, (θ)	IE %	WL, (g)	$\boldsymbol{C_R}$, (mm/Y)	Coverage surface, (θ)	IE %
0	0.82	622.4	--	--	0.78	19.9	--	--
100	0.81	615.3	0.011	1.1	0.75	18.9	0.049	5.0
300	0.67	512.1	0.177	17.7	0.65	16.4	0.176	17.6
600	0.54	412.8	0.337	33.7	0.56	14.2	0.287	28.7
900	0.52	396.0	0.364	36.4	0.54	13.7	0.310	31.0
1200	0.16	122.7	0.803	80.3	0.16	4.1	0.796	79.6
1600	0.12	94.4	0.848	84.8	0.13	3.4	0.829	82.9

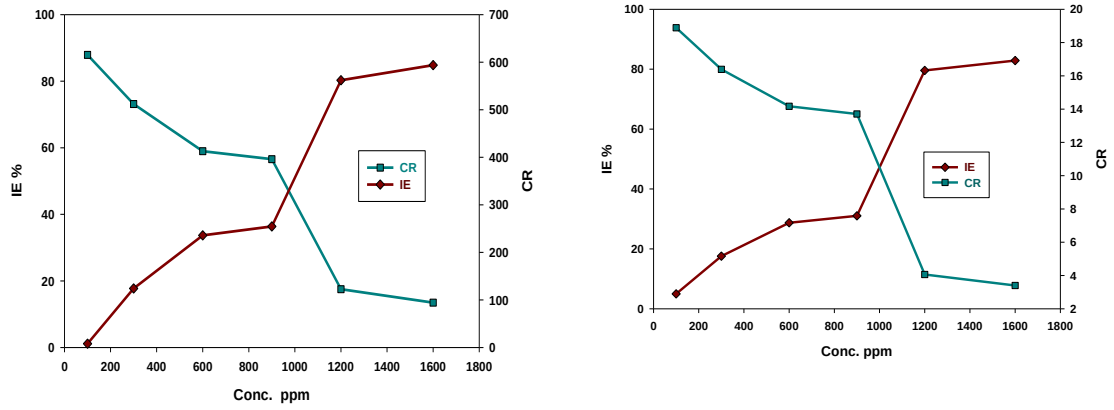

(a) (b)

Fig.2. The $\boldsymbol{C_R}$ values of inhibitor and inhibition efficiency (IE %) on Zn in 1M HCl with different concentrations of hybrid Ti/Ce salt at 25 °C after (a) 4 h, and (b) 120 h.

Fig. 2 provides the WL of the Zn after 4 h was maximum and inhibition reached after 120 h. In the beginning, the dissolution of the Zn took place due to the corrosive behavior of the acids. However, because of the dissolution the oxide layer that formed also took place on the metal surface. Thus, this oxide film remained intact and inert after 120 h leading to the passivation of Zn. On the contrary hybrid, Ti/Ce salt demonstrated inertness and passivation of Zn for a prolonged time thus happen corrosion prevention.

3.2. Effect of Time

Fig. 3. illustrates the immersion time effect on the corrosion of Zn in 1M HCl with different concentrations of hybrid Ti/Ce salt at 25 °C. The $\boldsymbol{C_R}$ values obtained from Zn WL in 1M HCl with different concentrations of hybrid Ti/Ce salt at

different immersion times are tabulated in Table 2. The C_R was decreased with an increase in immersion time till 120 h and then it becomes constant by adding an inhibitor concentration of 1600 ppm. In addition, the protection efficiency increased as immersion time increase. The protection efficiency values increase because of the protective film formed on the surface. The maximum inhibition efficiency reaches 82.9%.

3.3. Effect of Temperature

A temperature effect studied on the Zn immersed in 1M HCl without and existence of different concentrations of hybrid Ti/Ce salt for 1 h, as shown in Fig. 4. Table 3 gives the C_R values, coverage surface (θ), and inhibition efficiency (IE) of Zn in 1M HCl with 0, 100, 300, 600, 900, 1200, and 1600 ppm concentrations of hybrid Ti/Ce salt. The protection efficiency decreases with increases in the temperature of the electrolyte, which is compatible with previous studies [30]. It was found that there is an inverse relationship between the solution temperature and the corrosion resistance [31]. The temperature about 25 °C was the optimum temperature for the formation of a protective layer on the Zn surface.

Table 2. The C_R obtained from the WL of the Zn in 1M HCl with different of hybrid Ti/Ce salt concentrations at different immersion times.

Time, h	The concentration of inhibitor, ppm						
	0	100	300	600	900	1200	1600
0.5	1291.6	1462.2	792.0	1218.5	1212.4	243.7	121.9
1	1252.0	1257.6	1218.5	974.8	913.9	243.7	152.3
2	931.4	977.8	843.0	632.1	511.8	199.7	155.4
3	788.0	764.5	597.8	512.8	370.6	157.5	131.0
4	622.4	615.3	512.0	412.8	396.0	122.7	94.4
24	101.5	98.1	84.3	69.3	64.6	20.7	17.3
48	50.4	48.4	41.7	35.4	34.5	10.8	8.1
72	33.3	31.9	27.6	23.7	23.1	7.11	5.0
96	24.8	23.9	20.7	17.8	17.1	5.37	4.3
120	19.9	18.9	16.4	14.2	13.7	4.1	3.4

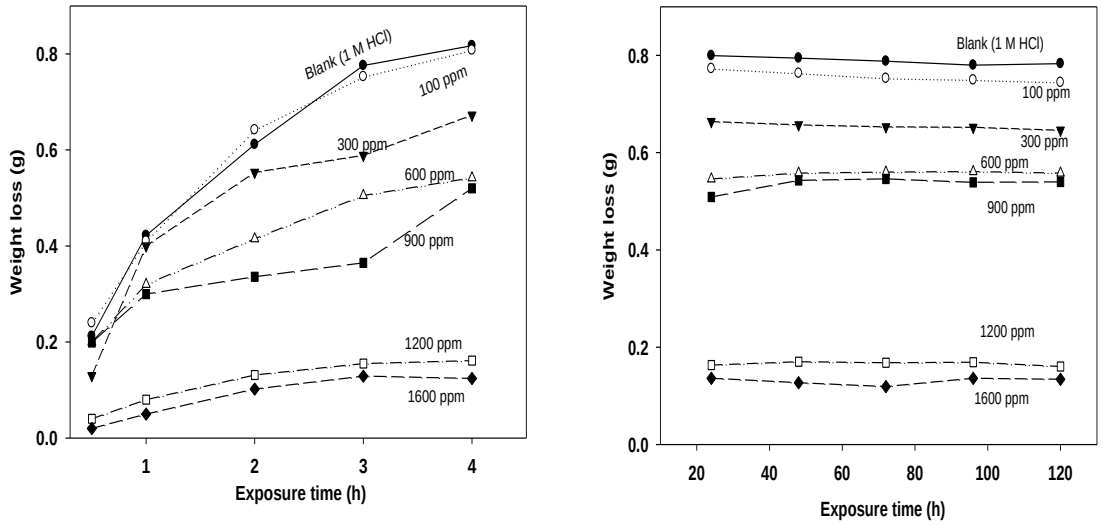

(a) (b)

Fig. 3. WL vs. immersion time for the Zn corrosion in 1M HCl with different concentrations of hybrid Ti/Ce salt at 25 °C after (a) 4 h, and (b) 120 h

Table 3. The C_R, Coverage surface (θ), and inhibition efficiency (IE%) of Zn in 1M HCl with different concentrations of hybrid Ti/Ce salt after 1 h immersed at different temperatures.

Conc. ppm	At 25 ^{0}C				At 55 ^{0}C			
	WL, (g)	C_R, (mm/Y)	Coverage surface, (θ)	IE %	WL, (g)	C_R, (mm/Y)	Coverage surface, (θ)	IE %
0	0.42	1294.4	--	--	0.62	1921.6	--	--
100	0.41	1257.6	0.028	2.8	0.46	1400.2	0.271	27.1
300	0.40	1226.9	0.052	5.2	0.45	1378.7	0.283	28.3
600	0.32	981.5	0.242	24.2	0.37	1133.3	0.410	41.0
900	0.30	920.2	0.289	28.9	0.34	1041.3	0.458	45.8
1200	0.08	245.4	0.810	81.0	0.25	762.2	0.603	60.3
1600	0.05	153.4	0.882	88.2	0.18	549.0	0.714	71.4

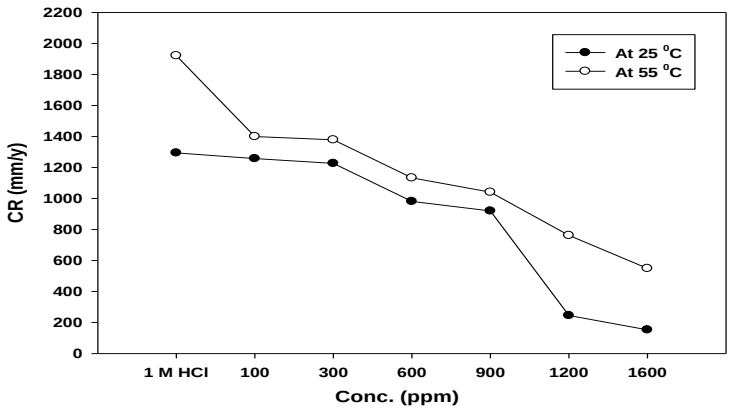

Fig. 4. The C_R of immersed Zn in 1M HCl without and existence of different of hybrid Ti/Ce salt concentrations after 1 h immersed at 25 °C and 55 °C.

3.4. Potentiodynamic polarization

The PDP plots for Zn in 1M HCl with different concentrations of hybrid Ti/Ce salt are given in Fig. 5. The corrosion potential (E_{corr}), anodic and cathodic Tafel slopes (βa, βc), corrosion current density (I_{corr}), polarization resistance (R_p), and inhibition efficiency (*IE %*), are listed in Table 4. The inhibitor concentration has a small effect on the anodic Tafel constant (βa) results and more effect on the cathodic Tafel constant (βc) values representing that the inhibitor might variation the mechanism of the cathodic reaction and may not affect the progression of anodic dissolution [32]. The parallel cathodic Tafel plots are attained in Fig. 5 which clear the hydrogen evolution is activation-controlled and the reduction mechanism is not affected by the inhibitor existence. The cathodic Tafel slope (β_c) values changes proposes that the reaction mechanism of the hydrogen reduction is different due to the existence or not of inhibitors. From Table 4, the data illustrate that the current density (I_{corr}) values decreased where the polarization resistance (R_p) values increased in the existence of various hybrid Ti/Ce salt concentrations as expected. The I_{corr} values of Zn in the inhibited solution are smaller than those for the inhibitor-free solution. This is because of the inverse relation between I_{corr} and R_p, with the increasing the inhibitor concentrations, the inhibitor molecules adsorption on the metal surface creates a physical barrier for both the mass and charge transfer, giving an excellent metal surface protection. The highest inhibition of those experiments value is 73 % at the 1600 ppm. The hybrid Ti/Ce salt addition led to shift the E_{corr} value to the negative direction. Moreover, the negative shift of corrosion potential provides that the studied compounds are mixed-type inhibitors but cathodic inhibitors than anodic ones [33]. The corrosion current density decrease, and the inhibition efficiency rise may be due to the compound's adsorption on the Zn surface. The experimental results derived from PDP curves show that in the existence of these compounds I_{corr} decreases significantly at all the studied concentrations. The Tafel polarization method confirmed the main WL data, providing some additional information. Thus, they are determined by the extrapolation of Tafel lines to the respective corrosion potentials.

Table 4. Corrosion parameters of the PDP curves for Zn in 1M HCl with different hybrid Ti/Ce salt concentrations

Inhibitor Conc. (ppm) 1 M HCl	E_{corr} mV	I_{corr} mA/cm^2	β_a mV/dec	β_c mV/dec	R_p ohm.cm^2	C_R, mm/y	Coverage surface, (θ)	IE %
0	-1019.0	7.8644	163.5	-174.4	3.40	91.98	--	--
100	-1026.8	4.7800	183.6	-197.6	6.37	55.90	0.392	39
300	-1017.2	3.7795	187.5	-199.5	8.18	44.20	0.519	52
600	-1028.6	3.4698	160.7	-195.0	8.20	40.58	0.558	56
900	-1023.9	3.2154	177.5	-194.3	9.20	37.60	0.591	59
1200	-1018.3	2.7798	185.9	-196.6	11.01	32.51	0.646	65
1600	-1026.8	2.1326	188.6	-199.1	14.41	24.94	0.728	73

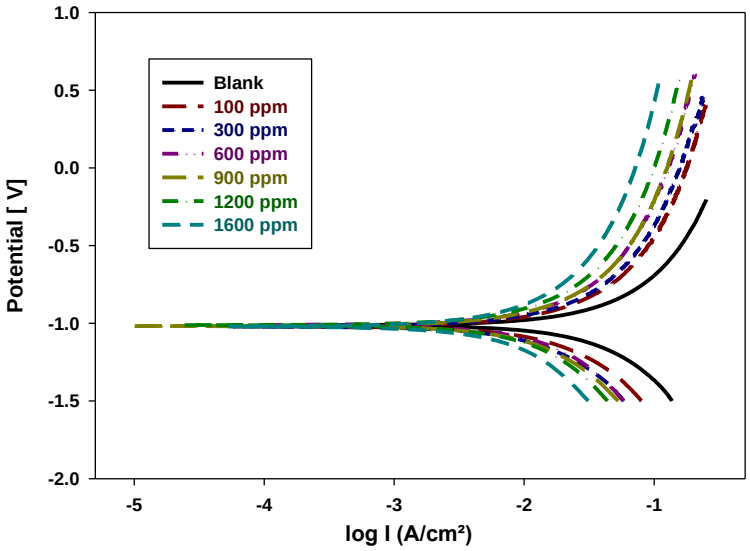

Fig. 5 The PDP curves for Zn in 1M HCl with different hybrid Ti/Ce salt concentrations.

The existence of Cl^- from HCl decrease by inhibitors due to chemisorptions mechanism that might be the cause by the water molecules evacuated from Zn surface share electrons between inhibitors heteroatom and Zn atom and thus the Zn surface might be adsorbed the inhibitor [34]. The corrosion mechanism of hybrid Ti/Ce salts in 1M HCl on Zn may be express by Eqs. (8-12) [21]:

$$Zn \rightarrow Zn^{2+} + 2e^- \quad (8)$$
$$O_2 + 4e^- + 2H_2O \rightarrow 4OH^- \quad (9)$$
$$Ce^{3+} + 3OH^- \rightarrow Ce(OH)_3 \quad (10)$$
$$4Ce^{3+} + O_2 + 4OH^- + 2H_2O \rightarrow 4Ce(OH)_2^{2+} \quad (11)$$
$$Ce(OH)_2^{2+} + 2OH^- \rightarrow CeO_2 + 2H_2O \quad (12)$$
$$Ce(OH)_3 \rightarrow Ce_2O_3 + 3H_2O \quad (13)$$
$$Ce^{3+} + H_2O_2 \rightarrow Ce^{4+} + OH^- \quad (14)$$
$$Ce^{4+} + 4OH^- \rightarrow Ce(OH)_4 \quad (15)$$
$$Ce(OH)_4 \rightarrow CeO_2 + 2H_2O \quad (16)$$

The Zn^{2+} cations are existed at the interface due to anodic reaction Eq. (8) while the hydroxyl anions that formed by oxygen reaction as in Eq. 9 (cathodic reaction). The Ce^{3+} cations form with OH^- anions $Ce(OH)_3$ and CeO_2 at the cathodic position as exist from Eqs. (10, 11, 12) that represent active sites blocking [19]. CeO_2 is a stable oxide that blocks the cathodic sites. From Eq. 10, it could be form Ce_2O_3 as in Eq. 13 [22]. It could also contain Ce^{4+} from Ce^{3+} then formation of $Ce(OH)_4$ that formed at last CeO_2 as from Eqs. (14, 15, 16) [22].

The electrochemical generation of the TiO_2 as in Eq. 17 where Eq. 18 gives the chemical dissolution of TiO_2 film. Finally, Eq. 19 provides the Ti chemical dissolution [35].

$$Ti + 2H_2O \rightarrow TiO_2 + 4H^+ + 4e^- \quad (17)$$
$$TiO_2 + 2H^+ \rightarrow TiO + H_2O \quad (18)$$
$$Ti + H_2O \rightarrow TiO^{2+} + 2H^+ + 2e^- \quad (19)$$

3.5. Surface morphology

The SEM image and EDX result of Zn before corrosion are seen in Fig. 6a and Fig. 6b, respectively. Also, the SEM morphology and EDX result of Zn immersed in 1 M HCl without additions are given in Fig. 6c and Fig.6d, respectively. The EDX analysis of Zn before corrosion is 100%Zn whereas the EDX result after corrosion in 1M HCl acid at 25 °C for 120 h is 27.79%O, 11.15%Cl, and 61.06%Zn. After time of immersion, the surface of pure zinc is uneven because it is mainly covered by flocculent corrosion products [36]. Also, it may be due to part of zinc is corroded in the solution with a pH below 6 [37].

The SEM images investigated the protective layer produced on the Zn surface. Fig 7. illustrates the SEM morphologies of the Zn immersed in 1 M HCl solution with the addition of hybrid Ti/Ce salt 100, 900, and 1600 ppm concentrations. Fig. 8 gives the EDX analyses of the six spots in Fig. 7. The EDX analyses of Spot 1 analysis are 25.88%O, 6.81%Cl, 0.24%Ti, 39.05%Zn, and 28.03%Ce and the EDX analysis for Spot 2 is 29.85%O, 10.87%Cl, 0.13%Ti and 57.84%Zn for 100 ppm hybrid Ti/Ce salt. Where for 900 ppm hybrid Ti/Ce salt, the EDX analysis for Spot 3 is 29.43%O, 11.58%Cl, 58.87%Zn, and 0.12%Ce while the EDX result for Spot 4 is 28.87%O, 12.01%Cl, and 59.12%Zn. Also, the EDX analyses for 1600 ppm of hybrid Ti/Ce salt for Spot 5 is 23.45%O, 12.49%Cl, 0.03%Ti, 59.98%Zn, and 4.05%Ce while for Spot 6 is 28.15%O, 12.69%Cl and 59.16%Zn.

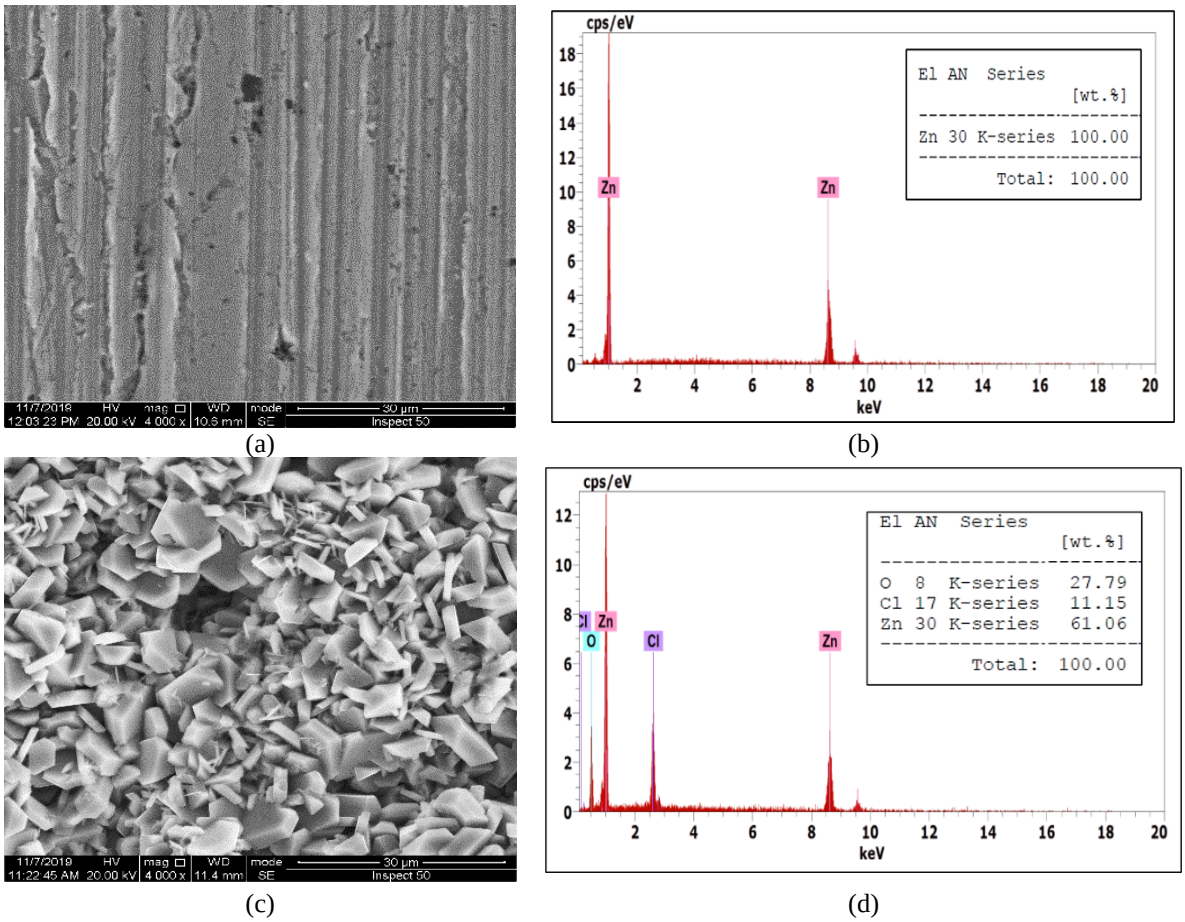

Fig. 6. The Zn (a) SEM before corrosion, (b) EDX before corrosion, (c) SEM of Zn immersed in 1 M HCl solution without additions at 25 °C for 120 h, and (d) EDX of Zn immersed in 1 M HCl solution without additions at 25 °C for 120 h.

The SEM images investigated the protective layer produced on the Zn surface. Fig 7. illustrates the SEM morphologies of the Zn immersed in 1 M HCl solution with the addition of hybrid Ti/Ce salt 100, 900, and 1600 ppm concentrations. Fig. 8 gives the EDX analyses of the six spots in Fig. 7. The EDX analyses of Spot 1 analysis are 25.88%O, 6.81%Cl, 0.24%Ti, 39.05%Zn, and 28.03%Ce, and the EDX analysis for Spot 2 is 29.85%O, 10.87%Cl, 0.13%Ti and 57.84%Zn for 100 ppm hybrid Ti/Ce salt. Where for

900 ppm hybrid Ti/Ce salt, the EDX analysis for Spot 3 is 29.43%O, 11.58%Cl, 58.87%Zn, and 0.12%Ce while the EDX results for Spot 4 is 28.87%O, 12.01%Cl, and 59.12%Zn. Also, the EDX analyses for 1600 ppm of hybrid Ti/Ce salt for Spot 5 is 23.45%O, 12.49%Cl, 0.03%Ti, 59.98%Zn, and 4.05%Ce while for Spot 6 is 28.15%O, 12.69%Cl, and 59.16%Zn. The existence of oxygen means the Zn is corroded and then formation of oxide layers which reduce further corrosion. The oxide film formation or corrosion products prevent the erosion of $Cl^-$and reduce the surface activity of zinc that led to decrease the $\boldsymbol{C_R}$ [36].

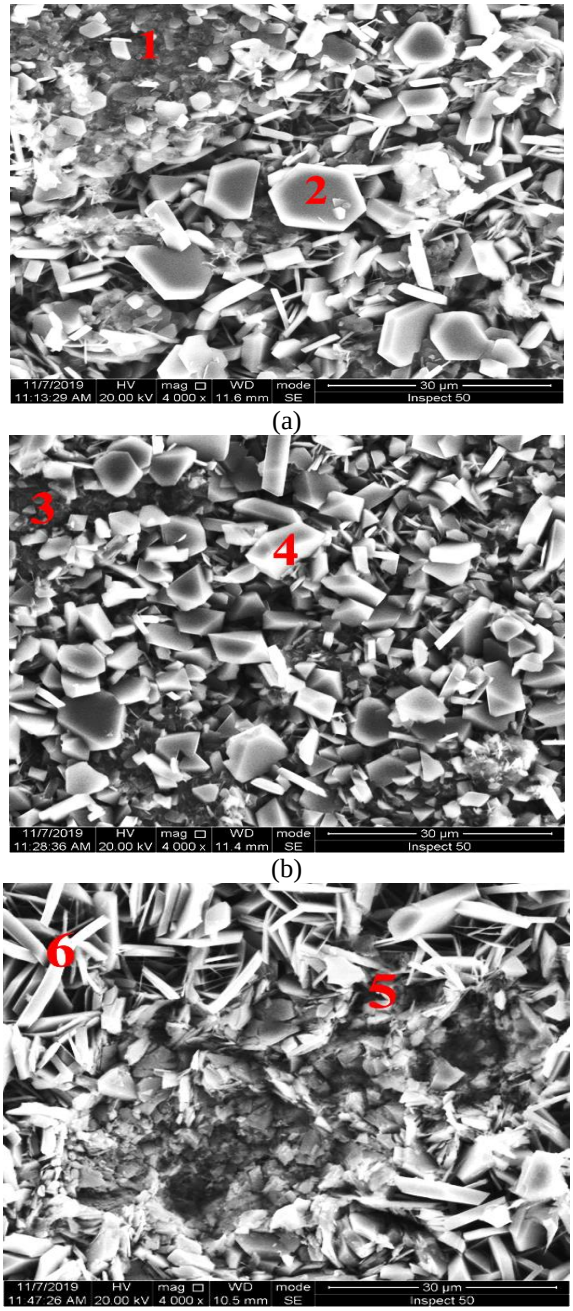

Fig. 7. The SEM morphologies of Zn immersed in 1 M HCl solution with additions of hybrid Ti/Ce salt at 25 °C for 120h (a) 100 ppm, (b) 900 ppm, and (C) 1600 ppm.

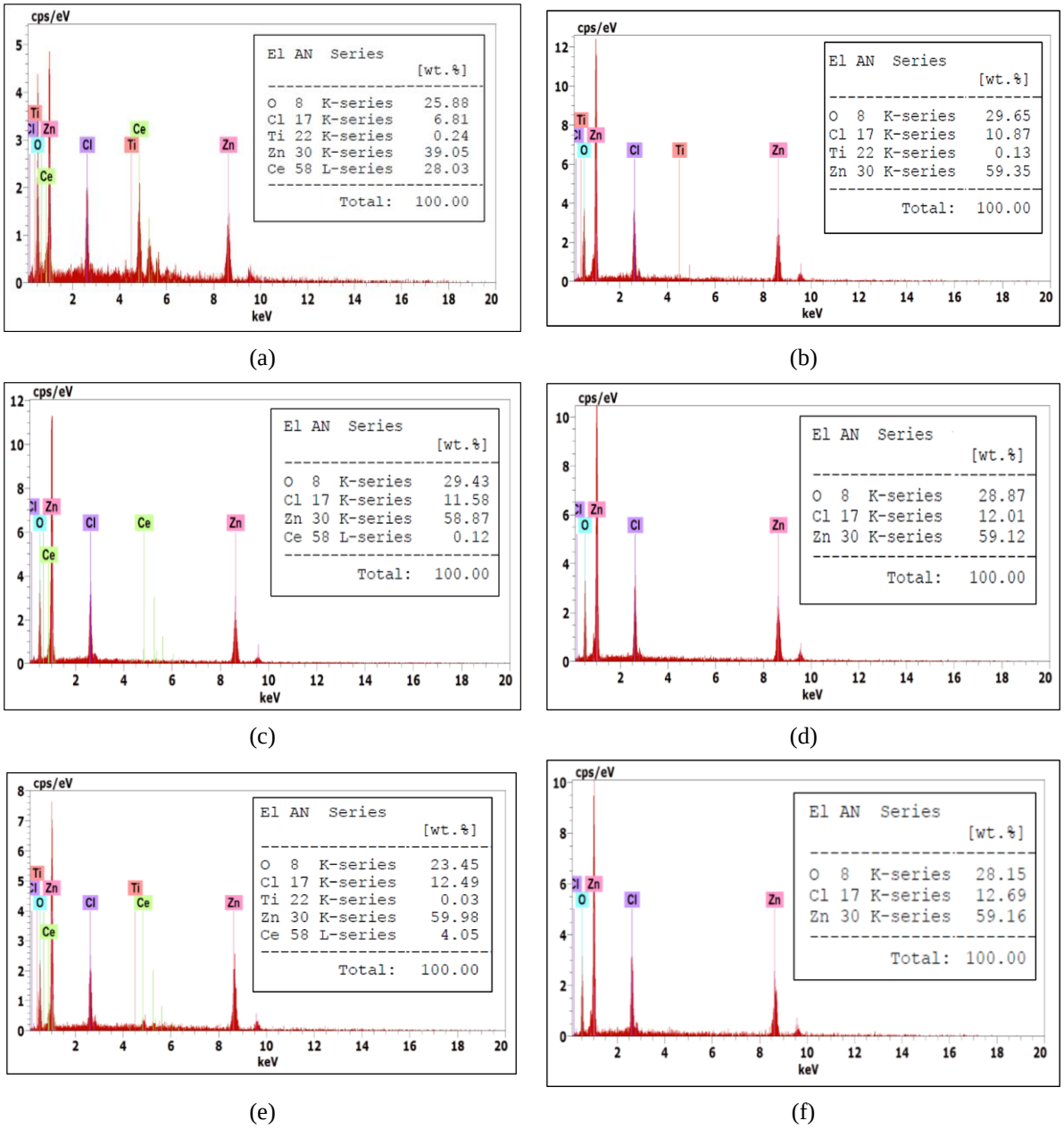

Fig. 8. The EDX analyses of Zn immersed in 1 M HCl solution with different additions of hybrid Ti/Ce salt at 25 °C for 120 h (a) Spot 1, (b) Spot 2, (C) Spot 3, (d) Spot 4 (e) Spot 5 and (f) Spot 6

Fig. 7(a) provides the SEM morphology of the Zn surface after immersion of 120 h which indicates small cavities on the surface. These are spread over the entire surface needle-like deposits are noticed. Where Fig. 7(b) displays more homogenous deposits on the Zn surface. In Fig. 7(c), it does not appear a needle-type of deposit. The protective film on Zn contains of a continuous amorphous-like layer in which several crystalline particles are embedded. From EDX analysis, the oxide film is a complex mixture of oxides of Ce and Zn. The yellow color of the oxide film formed on the Zn surface shows the existence of Ce^{4+} ions [13]. The formation of a protective film of hydrated Ce-rich oxide reduces the $\boldsymbol{C_R}$.

4. Conclusion

The corrosion inhibition on the Zn immersed in 1M HCl with 0, 100, 300, 600, 900, 1200, and 1600 ppm concentrations of hybrid Ti/Ce salts, different immersion time, different temperatures, and PDP curves were investigated. The protective layer was formed on the Zn surface due to the chelation reaction between Zn and inhibitor molecules decreasing the $\boldsymbol{C_R}$

by Ce^{3+} , Ce^{4+}, and Ti species. The inhibitors ions diffuse into the grain boundary of the Zn and contains a protective film. The lower $\boldsymbol{C_R}$ was exhibited by the Zn samples because of the surface coverage improvement by the addition of 1600 ppm of hybrid Ti/Ce. The inhibition efficiency raised with immersion time because of the protective film formation on the Zn surface. After 4 h, inhibition efficiency reached 82.9% and stabilized. The inhibition efficiency decreases slightly with increases the temperature due to the dissolution of Zn and the evolution of the hydrogen. The passive film formed on the Zn surface and confirmed by SEM images. Therefore, the prepared hybrid Ti/Ce modifies the Zn surface and gives good protection in 1M HCl solution.

Declaration of Competing Interest

There are no conflicts to declare.

Formatting of funding sources

The authors have no funding for this work.

References

[1] O. E. Oyeneyin, DFT and Monte Carlo Simulations on the Corrosion Inhibitive Potentials of some Furan-based Carbohydrazide Derivatives, Letters in Applied NanoBioScience, 12(4), 113, 2023

[2] M. S. Almahdy, A. F. Molouk, A. El-Hossiany, A. S. Fouda, Electrochemical Studies of Erica arborea Extract as a Green Corrosion Inhibitor for C-steel in Sulfuric Acid Medium, Biointerface Research in Applied Chemistry, 3(5), 2023, 472

[3] A. M. Guruprasad, H.P. Sachin, G.A. Swetha, B.M. Prasanna, Adsorption, and inhibitive properties of seroquel drug for the corrosion of zinc in 0.1 M hydrochloric acid solution Int. J. Ind. Chem., 10 (2019) 17–30

[4] M. Abdallah, I. Zaafarany, A.S. Fouda, and D. Abd El-Kader, Inhibition of Zinc Corrosion by Some Benzaldehyde Derivatives in HCl Solution, J. Mater. Eng. Perform., 21(6) (2012) 995-1002

[5] R.A. Prabhu, T.V. Venkatesha, B.M. Praveen, Electrochemical study of the corrosion behavior of zinc surface treated with a new organic chelating inhibitor ISRN Metallurgy, (2012)

[6] A. Prameswari, D. Dahlan, Y. Yetri, I. Imelda, A Corrosion Inhibition through the Adsorption of Cacao (Theobroma cacao) Peels Extract on Steel Surfaces: Experimental and DFT Results, Jurnal Ilmu Fisika, 15(1), 2023, 56–65

[7] K. A.saleh, K.S. Khalil, Corrosion inhibition of zinc in hydrochloric acid solution using Ampicillin, Iraqi J. Sci., 55(2A) (2014) 295-303

[8] S. Abd El Wanees, A.A.H. Bukhari, N.S. Alatawi, S.A. Khalil, S. Nooh, S.K. Mustafa, S.S. Elyan, , Thermodynamic and Adsorption studies on the corrosion inhibition of Zn by 2, 2'-Dithiobis(2,3-dihydro-1,3-benzothiazole) in HCl Solutions, Egypt. J. Chem., 64(2) (2021) 547 – 559

[9] H. M. Abd El-Lateef, M. EL Rouby, inhibition effect of poly(ethylene glycol) and cetyltrimethylammonium bromide on corrosion of Zn and Zn—Ni alloys for alkaline batteries, Trans. Nonferrous Met. Soc. China, 30 (2020) 259-274.

[10] S.K. Rajappa, T.V. Venkatesha, B. M. Praveen, Chemical treatment of zinc surface and its corrosion inhibition studies Bull. Mater. Sci., 31(1) (2008) 37–41.

[11] Y. K. Agarwal, J. D. Talati, M. D. Shah, M. N. Desai, N. K. Shah, Schiff bases of ethylenediamine as corrosion inhibitors of zinc in sulphuric acid, Corros. Sci., 46(3) (2004) 633–651.

[12] S. Manov, F. Noli, A. M. Lamazouere, L. Aries, Surface treatment for zinc corrosion protection by a new organic chelating reagent, J. Appl. Electrochem., 29(8) (1999) 995–1003.

[13] B. Muller, G. Imblo, Heterocycles as corrosion inhibitors for zinc pigments in aqueous alkaline media, Corros. Sci., 38 (1996) 293–300 .

[14] A. O. Alao, A. P. Popoola, M. O. Dada, O., Utilization of green inhibitors as a sustainable corrosion control method for steel in petrochemical industries: A review, Frontiers in Energy Research, 2023

[15] U. S. Nwigwe, C. I. Nwoye, The Efficacy of Plant Inhibitors as Used against Structural Mild Steel Corrosion: A Review, Portugaliae Electrochimica Acta 40 (2023) 381-395

[16] M Abdallah, SA Ahmed, HM Altass, IA Zaafarany, M Salem, AI Aly, EM Hussein, Competent inhibitor for the corrosion of zinc in hydrochloric acid based on 2, 6-bis-[1-(2-phenylhydrazono) ethyl] pyridine Chem. Eng. Commun., 206(2)(2019)137-148.

[17] M. Abdallah, Ethoxylated fatty alcohols as corrosion inhibitors for dissolution of zinc in hydrochloric acid, Corros. Sci., 45(12), (2003)2705- 2716.

[18] M. Abdallah, M. Alfaker, R.S. Abdel Hameed, Propoxylated Fatty Esters as Safe Inhibitors for Corrosion of Zinc in Hydrochloric Acid, Prot. Met. Phys. Chem. Surf., 56(1) (2020) 225-232.

[19] J. A. C. Mendez , J. d. P. Bueno, Y. M. Vong, B. P. Martínez, Cerium Compounds Coating as a Single Self-Healing Layer for Corrosion Inhibition on Aluminum 3003, Sustainability 2022, 14, 15056

[20] B. R. W. Hinton, L. Wilson, The corrosion inhibition of zinc with cerous chloride, Corros. Sci., 29(8) (1989) 967-985

[21] T. D. Nguyen, T. T. Pham, A. S. Nguyen, K. O. Vu, G. V. Pham, T. T. X. Hang, Inhibitory Effect of Benzoate-intercalated Hydrotalcite with Ce^{3+}-loaded clay on Carbon Steel, Corrosion Science and Technology, 22(1), (2023), 1-9

[22] L. Zhang, S. Huang, Y. Weng, J. Li, P. Han, S. Ye, X. Zhang, Preparation of Ni-P-Ti3C2Tx-Ce composite coating with enhanced wear resistance and electrochemical corrosion behavior on the surface of low manganese steel, Surface & Coatings Technology 441 (2022) 128508

[23] W. Liu, Z. Mo, C. Shuai, S. He, R. Yue, X. Guo, Y. Chen, H. Zheng, J. Zhu, R. Guo, N. Liu, Fabrication of TiO_2/CeO_2/PPS corrosion protective hydrophobic coating by air spraying, Colloids and Surfaces A: Physicochemical and Engineering Aspects 647 (2022) 129056

[24] V. R. Rathi, S. D. Nirmal, S. J. Kokate., Corrosion study of mild steel, tor steel and CRS steel by weight loss method, J. Chem. Pharm. Res., 2(2) (2010) 97-100.

[25] L.Z. Mohamed, M.A. H. Gepreel, A, Abdelfatah, Corrosion behavior of $Al_{12}Cr_{12}Fe_{35}Mn_{21}Ni_{20}$ high entropy alloy in different acidic media Chem. Pap., 75 (2021) 6265-6274

[26] A. Abdelfatah, A.M. Raslan, L.Z. Mohamed, Corrosion Characteristics of 304 Stainless Steel in Sodium Chloride and Sulfuric Acid Solutions, Int. J. Electrochem. Sci.,17 (2022) 220417

[27] G.A. Gaber, H.A. Aly, L.Z. Mohamed, Effect of Sodium Tungstate on the Corrosion Behavior of Fe-Base Alloy in H2SO4 Solution Int. J. Electrochem. Sci., 15 (2020) 8229–8240

[28] W. Tu, Y. Cheng, T. Zhan, J. Han, Ch Yingliang, Influence of Sodium Tungstate and Sealing Treatment on Corrosion Resistance of Coatings Formed on AZ31 Magnesium Alloy by Plasma Electrolytic Oxidation, Int. J. Electrochem. Sci., 12 (2017) 10863–10881

[29] M. Pais, P. Rao, An Up-to-Date Review on Industrially Signifcant Inhibitors for Corrosion Control of Zinc, Journal of Bio- and Tribo-Corrosion (2021) 7:117

[30] S.M. Ali, H.A. Al lehaibi, Control of zinc corrosion in acidic media: Green fenugreek inhibitor, Trans. Nonferrous Met. Soc. China, 26 (2016) 3034−3045

[31] H. S. Abdo, U. A. Samad, J. A. Mohammed, S. A. Ragab, A. H. Seikh, Mitigating Corrosion Effects of Ti-48Al-2Cr-2Nb Alloy Fabricated via Electron Beam Melting (EBM) Technique by Regulating the Immersion Conditions, Crystals 2021, 11, 889

[32] H. Gerengi, H. I. Sahin, S. lorentzii, Extract As a Green Corrosion Inhibitor for Low Carbon Steel in 1 M HCl Solution, Ind. Eng. Chem. Res., 51 (2012) 780–787.

[33] Z. Ghazi, H. ELmssellem, M. Ramdani, A.Chetouani, R. Rmil, A. Aouniti, C. Jama, B. Hammouti, Corrosion inhibition by naturally occurring substance containing Opuntia-Ficus Indica extract on the corrosion of steel in hydrochloric acid, J. Chem. Pharm. Res., 6(7) (2014) 1417-1425.

[34] N. Hossain, M. A. Chowdhury, M. Rana, M. Hassan, S. Islam, Terminalia arjuna leaves extract as green corrosion inhibitor for mild steel in HCl solution, Results in Engineering 14 (2022) 100438

[35] J. Hu, L. Chen, X. Zhong, S. Yu, Z. Zhang, D. Zeng, T. Shi, Corrosion Inhibition of Titanium in Hydrochloric Acid containing Na2MoO4, Int. J. Electrochem. Sci., 12 (2017) 8878 – 8891

[36] J. Feng, Y. Wang, X. Lin, M. Bian, Y. Wei, SECM in situ investigation of corrosion and self-healing behavior of trivalent chromium conversion coating on the zinc, Surface & Coatings Technology 459 (2023) 129411

[37] M. Pais, P. Rao, Green nanoparticles as a sustainable inhibitor to attenuate acid corrosion of zinc, Journal of Molecular Structure 1286 (2023) 135634